CISTER
Research Centre in
Real-Time & Embedded
Computing Systems

Conference Paper

Joint Spectrum and Antenna Selection Diversity for V2V Links with Ground Reflections

Ramiro Robles
Miguel Gutiérrez Gaitán
Gowhar Javanmardi
Harrison Kurunathan

CISTER-TR-240803

2024/10/21

Joint Spectrum and Antenna Selection Diversity for V2V Links with Ground Reflections

Ramiro Robles, Miguel Gutiérrez Gaitán, Gowhar Javanmardi, Harrison Kurunathan

CISTER Research Centre

Polytechnic Institute of Porto (ISEP P.Porto)

Rua Dr. António Bernardino de Almeida, 431

4200-072 Porto

Portugal

Tel.: +351.22.8340509, Fax: +351.22.8321159

E-mail: rsr@isep.ipp.pt, mjggt@isep.ipp.pt, gowha@isep.ipp.pt, jhk@isep.ipp.pt

https://www.cister-labs.pt

Abstract

This paper addresses the study of a fading-rejection algorithm based on joint spectrum and antenna selection in a vehicle-to-vehicle (V2V) multiple antenna system. The central objective of this selective scheme is to provide resilience against the destructive effects of the superposition of line-of-sight (LOS) and ground-reflected signals. The paper also provides an extension to channels that combine such deterministic superposition of multiple paths and reflections with an uncorrelated double scattering component, which shows how the algorithm is also beneficial under more general channel modelling assumptions. A multiple-ray performance model is used to describe the deterministic signal interactions between multiple antennas across contiguous vehicles. The antenna selection component is shown to reject deterministic fading, particularly at short values of the inter-vehicular distance. By contrast,when the spectrum bands are correctly chosen, the spectrum selection component can exhibit gains for a wider range of inter-vehicular distances than its antenna selection counterpart. This indicates that both components of the proposed solution are, in some cases, complementary, and therefore, they should be considered together in V2V multiple antennadesign. Derivation of the statistics of the selective scheme considering an additional double scattering stochastic channel component is here proposed. Simulation results from all expressions show important gains for a given range of inter-vehicular distances.

Joint Spectrum and Antenna Selection Diversity for V2V Links with Ground Reflections

Ramiro Robles[1], Miguel Gutiérrez Gaitán[1,2], Gowhar Javanmardi[1,3], and Harrison Kurunathan[1]

[1] CISTER Research Centre, Porto, Portugal
{rasro,mjggt,gowha,jhk}@isep.ipp.pt
[2] Pontificia Universidad Católica de Chile, Santiago, Chile
{miguel.gutierrez}@uc.cl
[3] Faculty of Engineering, University of Porto, Porto, Portugal
up202010875edu.fe.up.pt

Abstract. This paper addresses the study of a fading-rejection algorithm based on joint spectrum and antenna selection in a vehicle-to-vehicle (V2V) multiple antenna system. The central objective of this selective scheme is to provide resilience against the destructive effects of the superposition of line-of-sight (LOS) and ground-reflected signals. The paper also provides an extension to channels that combine such deterministic superposition of multiple paths and reflections with an uncorrelated double scattering component, which shows how the algorithm is also beneficial under more general channel modelling assumptions. A multiple-ray performance model is used to describe the deterministic signal interactions between multiple antennas across contiguous vehicles. The antenna selection component is shown to reject deterministic fading, particularly at short values of the inter-vehicular distance. By contrast, when the spectrum bands are correctly chosen, the spectrum selection component can exhibit gains for a wider range of inter-vehicular distances than its antenna selection counterpart. This indicates that both components of the proposed solution are, in some cases, complementary, and therefore, they should be considered together in V2V multiple antenna design. Derivation of the statistics of the selective scheme considering an additional double scattering stochastic channel component is here proposed. Simulation results from all expressions show important gains for a given range of inter-vehicular distances.

Keywords: MIMO · V2V · Line of sight · Two-Ray model

1 Introduction

Intelligent transportation systems (ITS) constitute one the best candidates to achieve future mobility and related sustainability goals in urban environments [5]. The performance of these systems depends on a highly reliable, real-time, and ultra-low latency vehicular network infrastructure [17]. The new 5G [18] and ITS standards [1] are expected to fulfill several of these infrastructure requirements.

One of the main features of 5G that will help in improving the reliability of wireless links is multiple antenna technology, also known as MIMO or multiple-input multiple-output systems. Multiple antennas will be located predominantly at the base stations (potentially on a large scale, i.e., massive MIMO) and in less quantity (due to implementation constraints) on the vehicle side. V2V (vehicle-to-vehicle) multiple antenna technology will also support connectivity, particularly when road infrastructure is unavailable or scarce. An additional reliability solution to MIMO has been recently considered for the vehicular connectivity problem: *dynamic and opportunistic spectrum management and allocation* [7]. The combined use of space and spectrum diversity will improve real-time V2X services. It will enable ultra-fast response for critical system control, thus leading to safer vehicular maneuvers and, in general, urban transport decision-making.

This paper attempts to contribute towards filling a gap in the literature of vehicular MIMO systems in scenarios with dominant deterministic channel components that experience the presence of explicit ground reflections. Our work analyzes the joint effects of antenna and spectrum band selection, considering frequency bands that are candidates in current standards to support vehicular connectivity.

By investigating the nulls and fade distributions of V2V systems based on the two-ray model, we obtain useful bounds and conclusions about the effects of joint antenna and spectrum selection on the following characteristics of the two-ray signal superposition model: *depth of the fades, density of fades,* and *path loss exponent transition*. We also include the study of the statistics of the selection algorithm when considering an additional stochastic channel component with double scattering features, which reveals that the proposed mechanism is also helpful in more generalized channel models. Summarizing, our contributions are the following:

1. Investigation of the properties of the interference channel due to ground reflections and the analysis of the effects of joint antenna and spectrum selection, and
2. Investigation of the statistics of the resulting SNR when considering deterministic ground reflections and double scattering distributions, which are typical of V2V scenarios. This is, to the best of our knowledge, a new type of derivation in the literature of V2V multiple antenna systems.

The rest of the paper is organized as follows. Section 2 presents a non-exhaustive review of related works. Section 3 presents the scenario and signal reception model for V2V links with multiple antennas. Section 4 introduces the fading characteristics of the two-ray model that will be relevant for analyzing the selection algorithm. Section 5 provides details of the proposed joint antenna and selective algorithm, including statistics of the resulting signal-to-noise ratio (SNR) when considering a double scattering stochastic component. Section 6 presents the results of our methods. Finally, Section 7 concludes the paper.

2 Related Work and Contribution

The characterization of V2V MIMO channels and the optimization of vehicular antenna design have gained the attention of research and industrial communities in the past few years, mainly due to the advent of vehicular intelligent networks.

V2V channels can be broadly divided into three groups: i) deterministic line-of-sight (LOS) models (e.g., [10]) that are useful for antenna separation and beam-forming problems, ii) deterministic multiple ground reflection ray tracing channels (e.g., [6,9]), and iii) geometry-based stochastic or stochastic vehicular channel models (e.g., [11]). Regarding antenna design, the majority of works have focused on three major issues: antenna position optimization (e.g., [15]), optimization of the number of antennas [8], or the problem of optimum antenna separation [10].

The literature of conventional MIMO has widespread use of antenna selection diversity [16]. Also, in conventional cellular networks, dynamic spectrum management has been used to extend cellular capacity, increase coverage, improve load-balancing in multi-cell scenarios, and provide an additional dimension for diversity combining. However, the use of these two combined technologies in V2V scenarios has yet to be reported to the best of our knowledge.

The work in [4] has presented a scheme to achieve diversity in V2V links with ground reflections using several fixed frequency bands. Our work follows the philosophy of this previous work and proposes an important upgrade. Instead of continuously using different fixed frequency bands, our work proposes a dynamic spectrum selection, where frequency bands are selected "on-the-fly" based on the available channel state information. The dynamic spectrum selection algorithm is combined with an antenna selection diversity scheme.

Contribution: Compared with previous works, our paper primarily looks at how the LOS (line-of-sight) component in a V2V MIMO system is affected by ground reflections and how we can fight against strong fading using a combined antenna and spectrum band selection mechanism. We prove that for different values of inter-vehicle distance, the dynamic allocation schemes contribute to improving the SNR (Signal-to-Noise Ratio) of the transceiver in different regimes: antenna selection has gains for short inter-vehicular distances. In contrast, frequency selection can be helpful for a wider range of inter-vehicular distances but always shorter than the critical point given by the total angle reflection (i.e., the main fade). Results of the statistics achieved by the selective algorithm when assuming an additional double-scattering component are here also provided under the assumption of uncorrelated double fading with a LOS component affected by ground reflections.

Notation: Scalar variables are denoted by lowercase letters. The variable i is the imaginary number $i = \sqrt{-1}$. Vector and matrix variables are denoted by lowercase and capital-bold letters, respectively. $|\cdot|$ denotes absolute value and vector norm operator. $f_Y(y)$, $F_Y(y)$, and $\bar{F}_Y(y)$ denote, respectively, the probability, cumulative, and complementary cumulative density functions of the random variable Y (PDF, CDF, and CCDF, respectively). Similarly, $\Psi_{Y|X}(i\omega)$

and $\Psi(i\omega)$ denote, respectively, the conditional and unconditional characteristic function (C.F.) of the random variable Y with respect to X.

3 System model

3.1 Scenario description

Fig. 1 depicts a V2V system where an antenna array is located on the rooftop of each vehicle [6]. The dimensions of the cars are identical, so the arrays in the two vehicles constitute a mirror image of each other. The distance between the two arrays, also called inter-vehicular distance, is denoted by d_{veh}. This means they are located at the same height (z_{ant}) with the same regular separation between antennas. The system assumes dynamic spectrum selection in different wavelengths λ_m, $m = 1, \ldots, M$. The main objective of this configuration is to select the antenna link and the spectrum band m that provide the best rejection of the fading effect that arises due to ground reflections and other impairments (e.g., scattering). This fading-rejection ability will be translated into improved reliability of future vehicular applications such as vehicle platooning and autonomous cars. Table 1 gives the list of main variables. The number of Tx antennas is denoted by N_{Tx}, while the number of receive antennas is denoted by N_{Rx}. The position of the jth transmit antenna is denoted by $\mathbf{r}_j^{(tx)} = [x_j^{(tx)}, y_j^{(tx)}, z_j^{(tx)}]$ while the position of the kth receive antenna is denoted by the vector $\mathbf{r}_k^{(rx)} = [x_k^{(rx)}, y_k^{(rx)}, z_k^{(rx)}]$. The direct distance between antenna j in the transmitter and antenna k in the receiver is denoted by $d_{j,k}$ and is given by [6]:

$$d_{j,k} = \sqrt{\left(x_j^{(tx)} - x_k^{(rx)}\right)^2 + \left(y_j^{(tx)} - y_k^{(rx)}\right)^2 + \left(z_j^{(tx)} - z_k^{(rx)}\right)^2}.$$

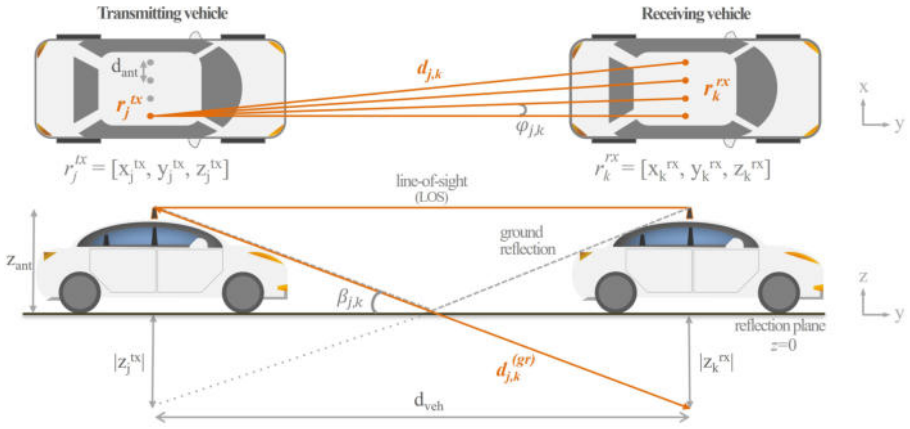

Fig. 1. V2V communication link: (bottom) LOS and ground reflected rays; and (top) an aerial view of the V2V channel [6]

Table 1. List of variables

Variable	Meaning
d_{veh}	Inter-vehicular distance
N_{Tx}	Number of Tx antennas
N_{Rx}	Number of Rx antennas
r	antennas position
$d_{j,k}$	Distance between jth Tx and kth Rx antennas
$h_{j,k,m}$	Channel between antenna j and antenna k in band m
$\Gamma_{j,k,m}$	Reflection coefficient between antennas j and k
λ_m	operational wavelength
$n_{gr,m}$	Complex refractive index in band m
c	light speed
$\epsilon_{r,m}$	Ground relative permittivity in band m
σ_m	Ground conductivity in band m
η	Signal to noise ratio
σ_v^2	Variance of noise
ϕ_Γ	Phase of reflection coefficient
P_T	Average Tx Power
κ	Modified Rice factor

The distance for the ground reflected ray, denoted by $d_{j,k}^{(gr)}$, is given by [6]:

$$d_{j,k}^{(gr)} = \sqrt{\left(x_j^{(tx)} - x_k^{(rx)}\right)^2 + \left(y_j^{(tx)} - y_k^{(rx)}\right)^2 + \left(z_j^{(tx)} + z_k^{(rx)}\right)^2}.$$

3.2 Channel model

The channel between the jth Tx antenna and the kth Rx antenna in the band m is denoted by $h_{j,k,m}$ and will be defined as the contribution of two components: the deterministic component that will include the LOS and ground reflections, and the second component that will consider all scattering contributions. This can be expressed as follows:

$$h_{j,k,m} = h_{j,k,m}^{(d)} + h_{j,k,m}^{(s)}, \tag{1}$$

where $h_{j,k,m}^{(d)}$ is the deterministic component of the channel and $h_{j,k,m}^{(s)}$ is the stochastic component. The ratio of the average power of the deterministic to the stochastic component is given by: $\kappa_{j,k,m} = \frac{|h_{j,k,m}^{(d)}|^2}{E[|h_{j,k,m}^{(s)}|^2]}$, and is called here modified Rice factor. The deterministic channel component $h_{j,k,m}^{(d)}$ will be described by the two-ray model. We consider the exact formulation of two rays traveling different distances and concurring at the same destination antenna. Each ray experiences path loss with an exponent equal to two (free space) and a phase shift delay proportional to the distance of each trajectory. This model assumes the two

rays arrive within the boundaries of a symbol duration (i.e., no inter-symbol interference). This can be expressed mathematically as follows [13]:

$$h_{j,k,m}^{(d)} = \frac{\sqrt{P_T}}{4\pi}(e^{2\pi i\tilde{d}_{j,k,m}}/\tilde{d}_{j,k,m} + \Gamma_{j,k,m}e^{2\pi i\tilde{d}_{j,k,m}^{(gr)}}/\tilde{d}_{j,k,m}^{(gr)}), \tag{2}$$

where P_T is the average total signal power including Tx and Rx antenna gains, $\tilde{d}_{j,k,m} = d_{j,k}/\lambda_m$ and $\tilde{d}_{j,k,m}^{(gr)} = d_{j,k}^{(gr)}/\lambda_m$, are respectively, the direct and the ground reflected electric distances between antenna j and antenna k in band m, $\Gamma_{j,k,m}$ is the reflection coefficient for the same tuple, and λ_m is the operational wavelength of the mth spectrum band. The reflection coefficient considering vertical polarization can be written as follows (modification of [3]):

$$\Gamma_{j,k,m} = \frac{n_{r,m}\sin\beta_{j,k} + B(\sqrt{n_{r,m}^2 - \cos\beta_{j,k}{}^2} + in_{i,m})}{n_{r,m}^2\sin\beta_{j,k} + (\sqrt{n_{r,m}^2 - \cos\beta_{j,k}{}^2} + in_{i,m})}, \tag{3}$$

where $\beta_{j,k,m}$ is the angle of reflection, $n_{r,m}$ is the real part of the complex refractive index of ground $n_{gr,m}$ and $n_{i,m}$ is the imaginary part of $n_{gr,m}$. For lossy materials we have $n_{gr,m} = n_{r,m} + in_{i,m} = \sqrt{\epsilon_{r,m} - i\frac{\sigma_m\lambda_m}{\epsilon_0 2\pi c}}$ [6], where c is light speed, while $\epsilon_{r,m}$ and σ_m denote, respectively, the relative permittivity and conductivity of asphalt pavement considering operation in the mth frequency band [14]. Regarding the stochastic component, it will be considered as a double scattering random variable, where each scattering component will be modeled as an independent circular complex Gaussian random variable: $h_{j,k,m}^{(s)} = x_{j,k,m}y_{j,k,m}$, where $\{x_{j,k,m}, y_{j,k,m}\} \sim \mathcal{CN}(0,\gamma)$, and γ is the variance of the zero-mean Gaussian random variable.

The signal-to-noise ratio (SNR) of a single antenna link (j,k) in frequency band m is thus given by:

$$\eta_{j,k,m} = \frac{|h_{j,k,m}|^2}{\sigma_v^2}, \tag{4}$$

where σ_v^2 is the noise variance.

4 Fading characteristics of the two-ray model ($\kappa \to \infty$)

First, let us investigate the characteristics of the V2V two-ray channel model that can be improved by the antenna and spectrum selection algorithm proposed in this paper. In the case of one Tx and one Rx antenna ($N_{Tx} = N_{Rx} = 1$), and considering dominance of the deterministic component in (1), which means κ is relatively large ($\kappa \to \infty$), the SNR expression in (4) boils down to the SNR of the conventional point-to-point two-ray model:

$$\eta = \tilde{P}_T\left|e^{i2\pi\tilde{d}_{los}}/\tilde{d}_{los} + \Gamma e^{i2\pi\tilde{d}_{gr}}/\tilde{d}_{gr}\right|, \tag{5}$$

where $\tilde{d}_{los}$ is the LOS electric distance, $\tilde{d}_{gr}$ is the electric distance of the reflected ray, and $\tilde{P}_T = P_T/(16\pi^2\sigma_v^2)$.

4.1 Depth of the fade

The fades are destructive interference patterns caused by the interaction between the direct and the ground reflection of the two-ray model in (5). These fades have different "depths", which can be defined as the minimum value achieved by the destructive interference. This depth in the two-ray model is bounded by:

$$\xi = 1 - |\Gamma(d_f)| \cos\beta(d_f), \tag{6}$$

where d_f is the distance of occurrence of the fade.

Proof Consider the normalized two-ray model, which is given by the ratio of the two-ray model in (5) to the free space loss:

$$\begin{aligned}\hat{\eta} = \eta/(\tilde{P}_T|e^{i2\pi\tilde{d}_{los}}/\tilde{d}_{los}|^2) &= |1 + \Gamma e^{i2\pi(\tilde{d}_{gr}-\tilde{d}_{los})}\tilde{d}_{los}/\tilde{d}_{gr}| \\ &= |1 + \Gamma\cos\beta e^{i2\pi(\tilde{d}_{gr}-\tilde{d}_{los})}| \\ &= |1 + |\Gamma|\cos\beta e^{i2\pi(\tilde{d}_{gr}-\tilde{d}_{los})+i\phi_\Gamma}|, \end{aligned} \tag{7}$$

where ϕ_Γ is the phase of the reflection coefficient. The fades occur when the two components in the previous equation cancel or considerably cancel each other. This happens when the second component achieves values closer to -1. Since $0 < |\Gamma| < 1$, $0 < \cos\beta \leq 1$, and both Γ and $\cos\beta$ are increasing functions with respect to the inter-vehicular distance, then the closest excursion of the second component in (7) to the value of -1 occurs when the phase of the exponential complex term is 180 degrees, which means $e^{2\pi(\tilde{d}_{gr}-\tilde{d}_{los})+\phi_\Gamma} = -1$. By substituting this value in the previous equation, we obtain the lowest excursion of the two-ray model or lowest bound on the depth of the fades:

$$\xi = 1 - |\Gamma(d_f)| \cos\beta(d_f),$$

where d_f denotes the distance at which the phase of the exponential term achieves the value to reach the bound on teh depth of the fade. This concludes the derivation of the depth of the fade in (6).

Corollary The fades of the two-ray model are never strictly null or zero. Their depth increases when the inter-vehicular distance increases or when the antenna height is reduced. They asymptotically reach null values for distances near the point where reflection conditions approach Brewster's total reflection criterion.

Proof Consider the expression in (6) for the depth of the fades of the two-ray model. The term $|\Gamma|$, or the reflection coefficient, only reaches the value of -1 for perfect metallic surfaces or for long distances between vehicles (i.e., beyond the distance given by Brewster's criterion for total internal reflection). For long distances, the value of $\cos\beta$ also tends to the value of 1. Therefore, the depth of the fades as described by (6) with $\Gamma \to -1$ and $\cos\beta \to 1$ asymptotically reaches a null value $\xi \to 0$ only when the distance is in the vicinity of the Brewster's total reflection distance.

4.2 Density of fades

The fades of the two-ray model occur at a variable frequency given by:

$$\nu = \frac{2\pi|\tilde{d}_{gr} - \tilde{d}_{los}| + \phi_{\Gamma}}{2\pi}.$$

For real values of the reflection coefficient (i.e., $\phi_{\Gamma} = 0$), the rate of fades of the two-ray model becomes

$$\nu = |\tilde{d}_{gr} - \tilde{d}_{los}|, \tag{8}$$

which means that at longer electric distances, where the difference between the two values $\tilde{d}_{gr}$ and $\tilde{d}_{los}$ is minimized, the rate of fades experienced by the receiver is reduced. By contrast, increasing the height of the antennas or reducing the inter-vehicular distance leads to an increased value of the difference between the two distances, which means an increase in the rate of appearance of fades.

Proof The proof follows from the analysis of the complex exponential term in (7). The fades occur when the second term (complex exponential) is as close as possible to -1, which occurs when the argument is equivalent to -180 degrees. The argument of the complex exponential term provides us with the angular and linear rate as follows:

$$e^{i2\pi\nu} = e^{i2\pi(\tilde{d}_{gr} - \tilde{d}_{los}) + i\phi_{\Gamma}}.$$

The value of the frequency is thus given by (8). This concludes the proof of the derivation of the rate of fades in (8).

5 Selection Diversity

5.1 Algorithm description

The main goal of this paper is to use the concept of diversity across antennas and spectrum bands to reduce the probability of fading that occurs with the interference created by ground reflections and/or scattering components. The idea behind this proposal is that not always processing all the available antenna links is beneficial for improved performance. There could be configurations of multiple antennas and spectrum bands that can experience deeper fades than other configurations. In our context, the joint spectrum and antenna selection algorithm can be expressed as an optimization problem:

$$\{j, k, m\}_{opt} = \arg_{j,k,m} \max |h_{j,k,m}|^2 . \tag{9}$$

5.2 Deterministic channels

From the results in the previous sections, we can predict some of the features of the selective algorithm. The maximum excursion of antenna link selection is given by the antennas at opposite ends of the vehicle width (v_w). This configuration

provides an effective distance difference with respect to two antennas facing each other given by $d_{dif} = \sqrt{\tilde{d}_{veh}^2 + \tilde{v}_w} - \tilde{d}_{veh}$. From this expression, we can observe that for larger values of d_{veh}, then $d_{dif} \to 0$ and the effects of maximum excursion of the antenna array decrease. Therefore, the effects of the multiple antenna systems (including antenna selection) also start to decline. This suggests that antenna selection is mainly beneficial for values of d_{veh} relatively short or small when compared to the vehicle width. This also means that path-loss transition beyond the critical point of total reflection is likely not to be influenced by antenna selection. The main fade given by the critical point is also expected not to be highly influenced by antenna selection, as this critical point mainly occurs at values of d_{veh} that are considerably large and therefore also larger compared to the vehicle width. By contrast, a change of frequency band can result in a more effective way to bring the electric vehicle width within values that can affect the location of the main fade. Therefore, we can select a set of frequency bands for which the maximum antenna excursion and spectrum dynamic selection can produce different fade distributions, allowing the selective algorithm to reject fades more effectively across different bands. This analysis will be verified in the section of results.

5.3 Stochastic channels

Let us now consider the case where the stochastic component in (2) becomes relevant, i.e. when κ increases. We consider that the stochastic component $h_{j,k,m}^{(s)}$ is described by a random variable with a strength characterized by a double Rayleigh distribution. The statistics of the SNR of the selected link and spectrum band as expressed by (9) can be obtained using the theory of order statistics [12]. This leads to the following PDF of the SNR of the proposed selection scheme:

$$f_{\eta^*}(y) = \sum_{j,k,m} f_{\eta_{j,k,m}}(y) \prod_{\{\hat{j},\hat{k},\hat{m}\} \neq \{j,k,m\}} F_{\eta_{\hat{j},\hat{k},\hat{m}}} \tag{10}$$

where $f_{\eta_{j,k,m}}(y)$ is the PDF of a single link with double scattering and with mean given by the deterministic channel component in (2). The CCDF (complementary cumulative distribution function) of this random variable can be calculated in integral-form as follows:

$$\bar{F}_{\eta_{j,k,m}}(y) = \int_{r=0}^{\infty} \sum_{n=0}^{\infty} \sum_{l=0}^{n} \frac{|\mu_{j,k,m}|^{2n} y^l}{n!(\gamma r)^{l+n}} e^{-\frac{y+|\mu|^2}{\gamma r}} \frac{1}{\gamma} e^{-\frac{r}{\gamma}} dr, \tag{11}$$

and as a proposed closed-form as follows:

$$\bar{F}_{\eta_{j,k,m}}(y) = \sum_{n=0}^{\infty} \sum_{l=0}^{n} \frac{|\mu_{j,k,m}|^{2n} y^l}{n!\gamma^{2l+2n}} 2 \left(\frac{y+|\mu|^2}{\gamma^2} \right)^{\frac{1-l-n}{2}} K_{l+n-1} \left(2\sqrt{\frac{y+|\mu_{j,k,m}|^2}{\gamma^2}} \right), \tag{12}$$

where $K_n(\cdot)$ is the modified Bessel function of the second kind and n-th order. The closed-form expression in (12) remains to be fully investigated as part of

our future work. For details in the derivation of these equations we refer to the Appendix. In practice, antenna selection can be activated when two connected vehicles have a good estimation of the average distance between them or when channel estimation allows the system to know accurate propagation conditions between vehicles. The objective of the selective antenna approach is to minimize the fading or destructive interference that is typical of two-ray model propagation and double scattering. By dynamically combining different locations of the receive and transmit antenna with the selection algorithm, the intention is to obtain less probability of low signal quality at the receiver end. Another advantage of antenna and spectrum selection is that the system is still characterized by a single link, rather than a combination of multiple components of the underlying multiple-input multiple-output system with multiple ground reflections.

6 Results

Consider a 2-vehicle configuration with $N = N_{Tx} = N_{Rx}$ antennas with variable distance between vehicles (d_{veh}). Each uniform linear array of antennas will be placed at a height given by $z_{ant} = 1.2$ meters. The width of the vehicles is set to $v_w = 1.5$ meters. Simulation settings are given in Table 2. Two operational frequencies are assumed to enable the spectrum band selection component: $f_1 =$ 3Ghz and $f_2 = 4$GHz. All the results are calculated using the same number of antennas on each vehicle side $N = 4, 8$, assuming vertical polarization for the reflection coefficient in (3). It is worth pointing out that all results assume a unitary Tx power $P_T = 1$ and unitary noise variance σ_v^2, which means that all SNR curves show the effective channel gain. It is, therefore, straightforward to scale the results to the desired power and noise levels according to the target bandwidth and spectrum band regulations.

The results in Fig. 2 show the individual SNR (channel gain) performance without antenna selection for the two targeted frequency bands. The figure also includes the solution for joint antenna and spectrum band selection (labeled as 'SEL'). We can observe that antenna selection rejects some of the fades, particularly for low values of inter-vehicular distance. This is observed in the curves that show modified peaks and fades on the left side of the figure. This ability to reject fades decreases as the inter-vehicular distance increases. This is because increased inter-vehicular distances yield a reduction in the diversity provided by the antenna arrays, as their performance becomes indistinguishable from a single antenna system for such long inter-vehicular distances. In turn, this means that for the largest channel fade, which is given by Brewster's total reflection critical point, the antenna selection system has reduced effectiveness, particularly when this critical distance point is relatively large compared to the width of the antenna array. In the case of the results in Fig.2, the main channel fade for both frequency bands occurs at distances beyond 25 meters, which is considerably large with respect to the width of the antenna arrays of only 1.5 meters. Therefore, we can observe that the antenna selection diversity scheme shows gains only for the first fades of the channel. By contrast, secondary frequency

Table 2. Simulation parameters

Variable	Meaning	value
d_{veh}	Inter-vehicular distance	1-50 (m)
z_{ant}	height of antenna array	1.5
v_w	vehicle width	1.5
ϵ_r	relative permittivity (asphalt) [14]	4
λ_1, λ_2	wavelengths	0.1m, 0.075m, (3GHz,4GHz)
σ	conductivity (asphalt) [14]	0.02
$h_{j,k,m}$	channel j,k antenna link in band m	(2)
N_{Tx}	Number of Tx antennas	8
N_{Rx}	Number of Rx antennas	8
P_T	Tx Power	Unitary

transmission provides a different channel fade distribution, which shows to be beneficial as the selective algorithm effectively removes the two main fades of the two spectrum bands. From our results in the previous sections, the fade density depends on the operational wavelength. Therefore, it is possible to select a set of channel frequencies with a fade distribution that can be complementary to each other (if possible). In the case of Fig. 2, we can observe that for values of the inter-vehicular distance close to the main channel fade or Brewster's total reflection angle, the two frequencies have a significant difference in the location of their main fade, and therefore, the dynamic spectrum allocation allows us to avoid the main channel fade of both frequencies. These results show how the combined diversity of spectrum and antenna selection will reduce the probability of fades, the depth of the fade, and also the density of the fades with respect to a single antenna V2V link.

The results in Fig. 3 show the cumulative distribution function (CDF) of the SNR (channel gain due to unitary Tx power and noise assumption) when considering a channel model with a stochastic component using a simulated version of the expressions previously derived. The results considered a modified Rice factor of $\kappa = 10$dB and used as a LOS component the multiple ray model for deterministic fading calculation as presented in (2). We can observe the gain provided by the joint selection of antenna and frequency band compared to the two CDFs of the individual bands with a single antenna transmission and ground reflection. This shows that the selection algorithm is also beneficial in channels with more general V2V channel models.

7 Conclusions

This paper has presented a scheme to achieve diversity in V2V channels by combining antenna and frequency band spectrum selection. In comparison with previous multiple antenna systems, the use of the spectrum band selection component to achieve additional diversity gains proves beneficial, particularly when

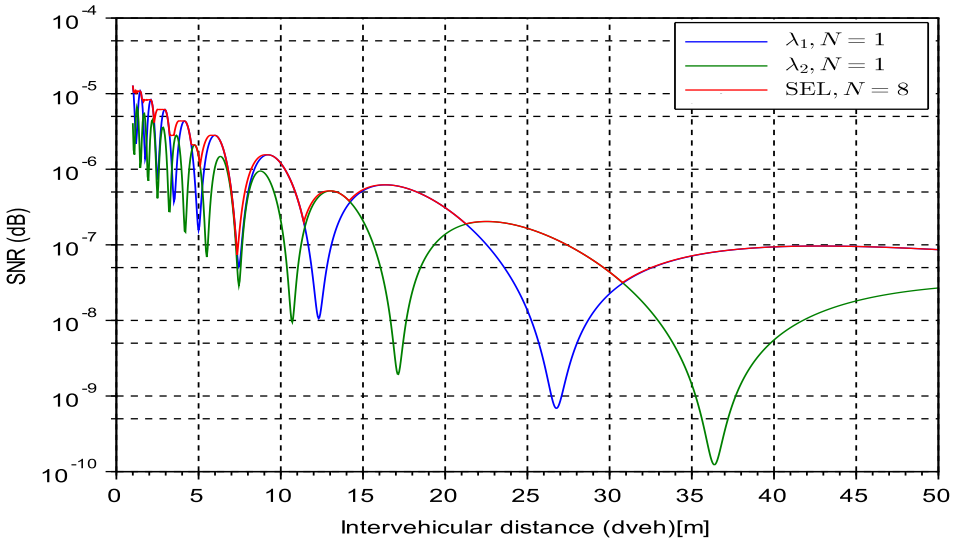

Fig. 2. SNR versus inter-vehicular distance (d_{veh} for different V2V schemes with or without antenna and spectrum selection (No scattering) assuming unitary noise and Tx power.

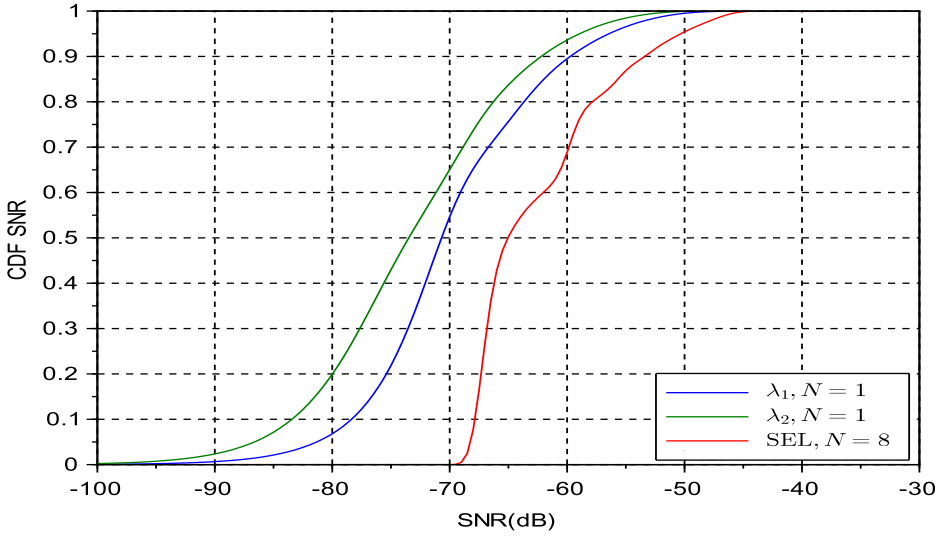

Fig. 3. CDF of the SNR for different V2V schemes with or without antenna and spectrum selection (Scattering).

the operational frequencies are not too dissimilar and when their fading distributions are complementary. We have proven using plots of the channel gain performance that antenna diversity is mainly beneficial for short values of inter-vehicular distance, while spectrum dynamic selection can provide rejection of channel fades when the selected frequency bands have distinct density of fades and also distinct locations of the main channel fade (total reflection). We have also shown that when considering a channel double scattering component, the cumulative distribution function (CDF) of the joint antenna and frequency band selection shows considerable improvements, which reveals additional gains. This means fades due to the stochastic signal superposition are also efficiently rejected together with the deterministic fading distribution. Expressions of the statistics were provided by considering uncorrelated double scattering stochastic components, which is to the best of our knowledge, a new attempt in the literature. Future work includes the investigation of selective schemes in the presence of outdated channel state information and in the presence of co-channel interference, which are problems that commonly arise in dynamic spectrum and opportunistic cognitive radio systems.

Acknowledgements This research was supported by FONDECYT Iniciación 11241221 and the Programa de Inserción Académica (PIA) from the Pontificia Universidad Católica de Chile; also by the CISTER Research Unit (UIDP/UIDB/04234/2020) by National Funds through FCT/MCTES (Portuguese Foundation for Science and Technology)and within project POCI-01-0145-FEDER-032218 (5GSDN); financed through National Funds from FCT and European funds through the EU ECSEL JU. **Note**: This document reflects only the author's view and the Commission is not responsible for any use that may be made of the information it contains. This work was also developed under project INSECT (ECSEL/0002/2019 - JU grant nr. 876038) also by FCT under PhD grant PRT/BD/154912/2023.

References

1. CEN/TC/278 , `https://www.itsstandards.eu/`, Accessed on February 14, 2024
2. Bateman, H., Erdélyi, A., Magnus, W., Oberhettinger, F.: Tables of integral transforms, vol. 1. McGraw-Hill New York (1954)
3. Besieris, I.M.: Comment on the "corrected fresnel coefficients for lossy materials". IEEE Antennas and Propagation Magazine **53**(4), 161–164 (2011)
4. Besser, K-L, J.E., Coon, J.: An efficient frequency diversity scheme for ultra-reliable communications in two-path fading channels. IEEE Journal of Communications and Networks (To appear) (2024)
5. Chen, J., Zhang, Y., Teng, S., Chen, Y., Zhang, H., Wang, F.Y.: ACP-based energy-efficient schemes for sustainable intelligent transportation systems. IEEE Transactions on Intelligent Vehicles (2023)
6. Farzamiyan, A.H., Gaitán, M.G., Sámano-Robles, R.: A multi-ray analysis of los V2V links for multiple antennas with ground reflection. In: 2020 AEIT International Annual Conference (AEIT). pp. 1–6. IEEE (2020)

7. Fu, B., Ren, J., Wang, G.: Dynamic optimal radio resource management scheme for V2V. In: 2019 International Conference on Artificial Intelligence and Advanced Manufacturing (AIAM). pp. 238–242. IEEE (2019)
8. Gaitán, M.G., Sámano-Robles, R., Farzamiyan, A.H.: On the optimum number of antennas for V2V los links with ground reflection. In: 2020 IEEE MTT-S Latin America Microwave Conference (LAMC 2020). pp. 1–3. IEEE (2021)
9. Gaitán, M.G., Samano-Robles, R., Rodriguez, J.: Outage probability of v2v multiple-antenna rice fading links with explicit ground reflection. In: GLOBECOM 2022-2022 IEEE Global Communications Conference. pp. 2656–2661. IEEE (2022)
10. Garcia, M.H.C., Iwanow, M., Stirling-Gallacher, R.A.: LOS MIMO design based on multiple optimum antenna separations. In: 2018 IEEE 88th vehicular technology conference (VTC-Fall). pp. 1–5. IEEE (2018)
11. Gutiérrez-Mena, J.T., Gutiérrez, C.A., Castillo, J.V.: Geometrical modeling of non-stationary double-rayleigh fading channels for mimo vehicle-to-vehicle communications. In: 2017 IEEE 9th Latin-American Conference on Communications (LATINCOM). pp. 1–6. IEEE (2017)
12. H. A. David, H.N.N.: Order Statistics. Wiley (2003)
13. Jakes, W.C., Cox, D.C.: Microwave Mobile Communications. Wiley-IEEE press (1994)
14. Jaselskis, E.J., Grigas, J., Brilingas, A.: Dielectric properties of asphalt pavement. Journal of materials in Civil Engineering **15**(5), 427–434 (2003)
15. Mirzaee, M., Adhikari, N., Noghanian, S.: Analysis of static and dynamic scenarios of MIMO systems for physical layer modeling for vehicular communication. In: 2014 National Wireless Research Collaboration Symposium. pp. 1–10. IEEE (2014)
16. Salhab, A.M., Zummo, S.A.: Outage performance of space diversity systems with Nth-best receive antenna selection and co-channel interference. In: 2014 IEEE International Conference on Communications (ICC). pp. 4916–4920 (2014). https://doi.org/10.1109/ICC.2014.6884099
17. Tang, Z., He, J., Yang, K., et al.: Matching 5G connected vehicles to sensed vehicles for safe cooperative autonomous driving. IEEE Network (2023)
18. Third Generation Partnership Project (3GPP): 5G System Overview, https://www.3gpp.org/technologies/5g-system-overview, Accessed on June 17, 2024

Appendix Derivation of statistics of the joint antenna-frequency selection in Eq.(11) and (12).

Consider a random variable given by

$$y = \mu + xz, \tag{13}$$

where μ is the mean and x, y are both zero-mean circular complex Gaussian random variables with variance γ. The random variable $\nu = |y|^2$ is therefore considered here as a random variable with a LOS component and with double scattering. Consider now the characteristic function (CF) of this random variable conditional on a given value of the r.v. $r = |x|^2$, which leads to the conventional Rice CF as follows:

$$\Psi_{\nu|r}(i\omega) = \frac{1}{1 - i\omega\gamma r} e^{\frac{i\omega|\mu|^2}{1-i\omega\gamma r}}, \tag{14}$$

which can be rewritten as follows:

$$\Psi_{\nu|r}(i\omega) = \frac{1}{1-i\omega\gamma r} e^{-\frac{|\mu|^2}{\gamma r}} e^{\frac{|\mu|^2/\gamma r}{1-i\omega\gamma r}} = e^{-\frac{|\mu|^2}{\gamma r}} \sum_{n=0}^{\infty} \left(\frac{|\mu|^2}{\gamma r}\right)^n \frac{1}{n!(1-i\omega\gamma r)^{n+1}}.$$

The back-transform of this expression yields the following conditional CCDF:

$$\bar{F}_{\nu|r}(y) = \sum_{n=0}^{\infty} \sum_{l=0}^{n} \frac{|\mu|^{2n} y^l}{n!(\gamma r)^{l+n}} e^{-\frac{y+|\mu|^2}{\gamma r}}$$

The unconditional CCDF of ν can be obtained as follows:

$$\bar{F}_{\nu|r}(y) = E_r[\bar{F}_{\nu|r}(y)] = \int_{r=0}^{\infty} \bar{F}_{\nu|r}(y) f_r(r) dr, \tag{15}$$

where $f_r(r) = \frac{1}{\gamma} e^{-\frac{r}{\gamma}}$. This can be expressed explicitly as follows:

$$\bar{F}_{\nu}(y) = \int_{r=0}^{\infty} \sum_{n=0}^{\infty} \sum_{l=0}^{n} \frac{|\mu|^{2n} y^l}{n!(\gamma r)^{l+n}} e^{-\frac{y+|\mu|^2}{\gamma r}} \frac{1}{\gamma} e^{-\frac{r}{\gamma}} dr. \tag{16}$$

Let us now use the following change of variable $u = \frac{r}{\gamma}$ in the previous expression, which yields:

$$\bar{F}_{\nu}(y) = \int_{u=0}^{\infty} \sum_{n=0}^{\infty} \sum_{l=0}^{n} \frac{|\mu|^{2n} y^l}{n!(\gamma^2 u)^{l+n}} e^{-\frac{y+|\mu|^2}{\gamma^2 u}} e^{-u} du, \tag{17}$$

which yields, using formula (29) in Chapter 4.5 of the integral tables in ([2]), the following:

$$\bar{F}_{\nu}(y) = \sum_{n=0}^{\infty} \sum_{l=0}^{n} \frac{|\mu|^{2n} y^l}{n!\gamma^{2l+2n}} 2 \left(\frac{y+|\mu|^2}{\gamma^2}\right)^{\frac{1-l-n}{2}} K_{l+n-1}\left(2\sqrt{\frac{y+|\mu|^2}{\gamma^2}}\right), \tag{18}$$

where $K_n(\cdot)$ is the nth order modified Bessel function of the second kind. This final expression remains to be confirmed as part of future work. This concludes the derivation of (11) and (12) in the integral form and in its potential closed-form expression.